Photovoltage Enhancement: Analysis of Polaron Formation and Charge Transport at the Junctions of Organic Polythiophene and Inorganic Semiconductors†

Alexander D. Q. Li* and Lin Song Li

Department of Chemistry, Washington State University, Pullman, Washington 99164

Received: December 31, 2003; In Final Form: June 3, 2004

We report the charge transport properties at the junction of organic polythiophene (PT) and inorganic semiconductors. Using a Kelvin probe and surface photovoltage spectroscopy, we have found that excitation of inorganic semiconductor band gaps led to hole migration across the inorganic−organic interface (IOI) and subsequently creation of polaron states in PT polymer chains. Of particular interesting is that these polaron states yield photovoltage responses initially at 675 nm, and eventually over the entire region of the visible spectrum. Because of their long lifetime (hours to days), the density of these polaron states increases with the exposure time of photoexcitations of the inorganic semiconductor until saturation is reached. The net result is that photovoltage is enhanced over the visible spectrum through charge transfer of polaronlike states in PT to inorganic semiconductors. Sunlight can induce obvious photovoltage enhancement at these IOI junctions, which show potential promise in the future application of large area photovoltaic technology.

Introduction

Conversion between photonic energy and electronic energy is technologically important and provides ample opportunities to study fundamental physical phenomena such as photoinduced charge transfer. Recently, we have experienced rapid growth of light emitting diodes (LED), in particular organic and polymeric electroluminescence materials, which have the potential promise of future large-area displays. The essence of electroluminescence phenomena is converting electronic energy to photonic energy. Conversely, the photovoltaic effect harvests photonic energy and converts it to electronic form in solar cells. Both fields benefit greatly from the recent advancement in conjugated polymers and their self-organization properties.[1−7]

While interest in pure organic photovoltaic cells grows, studies of solar cells made of nanostructured materials and hybrid inorganic and organic materials are also advancing rapidly due to their obvious technological potentials.[8−12] For instance, Grätzel and co-workers[8,9] have reported dye-sensitized solar cells with solar conversion efficiency as high as 10%. Such a "Grätzel cell" uses TiO_2 electrodes and popular Ru bipyridyl or porphyrin derivatives as photosensitizers. The most recent efforts in dye-sensitized TiO_2 solar cell research focus on replacing the liquid electrolyte with solid-state polymeric materials.[10] As a result, there has been great interest in photoinduced electron transfer in hybrid solar cells based on inorganic nanocrystals and conjugated polymers.[13−19] For example, Carter et al.[16] studied the effects of polymer thickness, morphology, and hole mobility on a photovoltaic device consisting of an optically active layer of poly(2-methoxy, 5-(2′-ethyl-hexyloxy) -*p*- phenylenevinylene) and TiO_2 exciton dissociation layer sandwiched between ITO and Au electrodes. Their results have shown that thin polymer layers with high carrier mobility on rough TiO_2 surface lead to the most efficient collection of photogenerated carriers. Quantum efficiencies of 6%, open circuit voltage of 1.1 V, and current densities of 0.4 mA/cm^2 were achieved at the maximum absorption of the polymer with large-surface-area TiO_2 layers as a semitransparent electrode. Rectification ratios greater than 10^5 under 100 mV/cm^2 white light illumination and fill factors as high as 69% at low light intensities were obtained.[16]

To enhance photovoltage and photocurrent, current research directions aim at developing new sensitizers, improving interfacial energetics, and suppressing charge recombinations.[20,21] These desired characteristics are intrinsically connected to the nanostructures and the order of materials. Regioregular (RR)-substituted polythiophene (PT) polymers such as *p*-type poly(3-alkylthiophene) (P3AT), for example, can form nanocrystalline lamellae thin films with their alkyl chains normal to the substrate, resulting in relatively high hole mobilities of 0.1 $cm^2V^{-1}S^{-1}$.[6,7] However, stereo regiorandom P3AT films do not show such an ordered structure, and their hole mobility is as low as 10^{-5} $cm^2V^{-1}S^{-1}$. Therefore, thin film transistors with RR P3AT have been used to fabricate integrated circuits, organic light-emitting diodes, and solar cells.[6,7,22,23] Conversely, metal oxides have a relatively large density of surface states, which yield very rich interfacial charge-transfer phenomena.[18] In addition, metal oxides exhibit extremely rich electronic properties, ranging from insulators, semiconductors, and conductors, to superconductors. Understanding charge-transfer mechanisms at the junction of metal oxides and conjugated polymers underpins common physics governing both LED devices and solar cells. Therefore, we hope to gain intrinsic information about charge transfer behaviors across inorganic organic interfaces (IOI), *p*−*n* junctions of P3AT, and inorganic semiconductors, and provide further guidance in the design of solid-state solar cells.

To monitor charge transfer across the IOI junction, we employ surface photovoltage (SPV) and surface photovoltage spectroscopy (SPS), which measure those optical absorption bands followed by charge transfer across the interface. These are the optical absorption bands that contribute to the photovoltaic

† Originally submitted for the "Alvin L. Kwiram Festschrift", published as the June 24, 2004, issue of *J. Phys. Chem. B* (Vol. 108, No. 25).

* To Whom Correspondence should be addressed. E-Mail: dequan@wsu.edu.

10.1021/jp0380576 CCC: $27.50
Published on Web 08/04/2004

effect. SPV and SPS are very sensitive tools for studying the change of charge distribution on semiconductor surfaces, buried interfaces, and heterojunctions.[24−29] Therefore, SPV and SPS are especially versatile for investigating charge-transfer phenomena at the IOI or in photovoltaic devices.

The recent advances in polymer photonics and optoelectronic devices, such as light emitting diodes, thin-film field-effect transistors, and solar cells,[1−6] have led to intense studies of charge transport at the interfaces of organic polymers and inorganic metal oxides. The focus has been on improving optoelectronic properties and power efficiency, and understanding electron, hole, or exciton transport properties in the conjugated polymers.[5,6] In this paper, we have constructed many *p*−*n* junctions using an organic semiconductive regioregular (RR) poly(3-alkylthiophene) (P3AT) and inorganic semiconductors (e.g., TiO_2, ZnO, and CdS) and investigated photoinduced charge transfer at their IOI junctions.

Experimental Section

Inorganic Substrate Preparations. The conductive ITO substrates (sheet resistance $R_s \leq 40\ \Omega/$) were purchased from Delta Technologies Company. Before each deposition, ITO substrates were first ultrasonically cleaned in an acetone and then rinsed in deionized water, followed by drying under N_2. TiO_2/ITO, ZnO/ITO, $BaTiO_3$/ITO, $SrTiO_3$/ITO, CdO/ITO, and HfO_2/ITO substrates were fabricated using the chemical solution deposition method. Formation of metal oxide films is confirmed by X-ray diffraction results. Specific procedures for preparing metal oxide thin films are as follows.

CdO Films on ITO. Cadmium nitrate tetrahydrate (Acros, Fisher Scientific Co.) was dissolved in water to make a 20 wt % aqueous solution. It was then mixed with an aqueous poly(vinyl alcohol) (PVA, from Aldrich Chemical Co) solution containing 10 wt % PVA at a weight-to-weight ratio of 2:1 to yield a homogeneous metal salt-polymer solution. Metal salt-polymer composite films were obtained by spin coating this solution onto ITO substrates at a spinning speed of 3000 rpm. The composite films were heated to 550 °C for 1.5 h to yield cadmium oxide film on ITO substrates. X-ray diffraction confirmed the formation of crystalline CdO films with Bragg diffraction peaks at 33.0, 38.2, 55.2, and 65.8°, which correspond to the miller index of (111), (200), (220), and (311), respectively.

TiO_2/ITO, ZnO/ITO, and HfO_2/ITO Films. All other metal oxide films were made similarly to the CdO described above by first preparing a 20 wt % aqueous solution of the metal oxide precursors. The metal oxide precursors used were titanium(IV) bis(ammonium lactato)dihydroxide, (50 wt % solution in water, from Aldrich Chemical Co), zinc nitrate (hydrate, 99.999%, from Aldrich Chemical Co), and hafnium chloride (98%, from Aldrich Chemical Co). The metal precursor solutions were then mixed with 10% (w/w) PVA at a weight ratio of 2:1 to yield a homogeneous metal salt-polymer solution. The spin-coating parameters and firing conditions are similar to the above descriptions for CdO/ITO films. X-ray diffraction confirmed the formation of various crystalline metal oxide films on ITO substrates. TiO_2 (anatase phase), $2\theta°$ (*hkl*): 25.2 (100), 37.8 (004), 48.0 (200), and 55.0 (211). ZnO, $2\theta°$ (*hkl*): 31.3 (100), 34.2 (002), and 36.1 (101). HfO_2, $2\theta°$ (*hkl*): 28.3 (111), 31.7 (111), and 34.6 (020).

Mixed Metal Oxide Thin Films. $BaTiO_3$/ITO and $SrTiO_3$/ITO were made by a mixture of titanium(IV) bis(ammonium lactato)-dihydroxide with barium acetate (99%, from Aldrich Chemical Co) or strontium nitrate (99+%, from Aldrich Chemical Co) at a molar ratio of 1: 1 in water solution containing 20% metal salt by weight. Then, the binary metal solutions were mixed with the PVA solution (10 wt %) at a weight ratio of 2:1 to yield a homogeneous Ba−Ti or Sr−Ti salt-polymer solution. The spin-coating parameters and firing conditions are similar to the above descriptions for CdO/ITO films. X-ray diffraction confirmed the formation of crystalline ABO_3-type metal oxide films. $BaTiO_3$, $2\theta°$ (*hkl*): 31.3 (110), 38.6 (111), and 45.0 (200). $SrTiO_3$, $2\theta°$ (*hkl*): 32.5 (110), 39.6 (111), and 46.2 (200).

CdS/ITO Films. The CdS/ITO thin films were made exposing of CdO/ITO films to H_2S gas. About 2 mg of thioacetamide (Acros, Fisher Scientific Co.) was added to a container, in which the cadmium oxide film is placed. After sealing the container with a rubber stopper, about 1 mL H_2O was injected into the container to initiate the slow release of H_2S by the reaction between thioacetamide and H_2O. After more than 1 h, orange CdO films are converted to yellow CdS films. The average thickness of inorganic films was controlled to around 100 nm as measured by a profilometer.

Self-Assembled Polymer Multilayers. Regioregular (*RR*) substituted poly(3-alkylthiophene), poly(styrene sulfonate) (PSS), and poly(diallydimethylammonium) (PDDA) were purchased from Aldrich and used without further purification. As negatively or positively charged polymers, PSS and PDDA were used to prepare selfassembled layer pairs in an alternative manner. The aqueous concentration of PDDA or PSS polymer was 10 mM. Because TiO_2 thin-film surfaces bear positive charges, we started the multilayer deposition with the negatively charged polymer PSS. Immersing the TiO_2/ITO substrate in the PSS solution for about 5 min, a PSS monolayer is formed due to the electrostatic attractive force between the negatively charged PSS polymer and the positively charged TiO_2 surface. The coated sample was then washed with deionized water to remove all of the nonadsorbed materials. The formation of PSS−PDDA layer pairs is accomplished by immersing PSS-coated TiO_2/ITO substrate in a PDDA aqueous solution for another 5 min, followed by washing with deionized water. Repeating the above steps, additional layer pairs of PDDA and PSS were deposited and a polymer multilayer structure on the TiO_2/ITO substrate was constructed.

Formation of Polythiophene and Metal Oxide Junctions. The formation of inorganic and organic *p*-*n* junctions was fabricated by spin coating polythiophene, for example, PT(4): poly(3-butylthiophene), PT(8): poly(3-octylthiophene), and PT-(12): poly(3-dodecylthiophene), on the various substrates prepared as described above. This results in junctions of *p*-type polymers on *n*-type metal oxides such as TiO_2, as well as junctions consisting of *p*-type polymers, insulating PSS/PDDA layer pairs, and *n*-type metal oxides (i.e., *p*−I−*n* junctions).

Kelvin Probe Measurements. A commercial Kelvin probe system (KP-6500 Digital Kelvin Probe System, McAllister Technical Services) was integrated with a light source to determine the work function changes when metal oxide films were modified with polymer layers. This apparatus measures the contact potential difference (CPD) between a reference plate and the sample's surface. CPD is defined as the work function of the reference plate connected to the preamplifier minus the work function of the sample,that is, $\Phi_m - \Phi_{sam}$ (where Φ_m is the work function of the reference plate (a constant), and Φ_{sam} is the work function of the sample). By comparing the work function before and after deposition of P3AT onto a TiO_2/ITO substrate, the change in work function, $\Delta\Phi$, after the deposition is obtained. The probe plate is made of stainless steel with a diameter of 2 mm. It was electrically connected via ground to the sample during the measurement. The typical distance

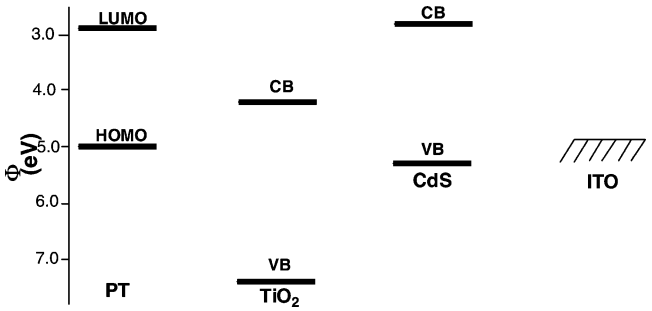

Figure 1. Energy diagram relative to vacuum for PT (LUMO: lowest unoccupied molecular orbital; HOMO: highest occupied molecular orbital), TiO_2 (VB: valence band; CB: conduction band), and ITO (From Arango et al.[15] and Breeze et al.[17]).

between the reference plate of the probe and the sample was less than ~1 mm. The oscillation frequency of the probe was 100 Hz. The measurement has an accuracy of 2.5 mV and was typically performed under ambient conditions.

Surface Photovoltage Spectroscopy (SPS). For SPV response, the samples were illuminated from the backside of transparent substrate by monochromatic light, which was obtained by passing light from a 450-W xenon lamp through a double-prism monochromator (SPEX FL3-21). Photoinduced SPV spectra were obtained by scanning the wavelength of the incident light from the visible to UV range (250−800 nm) at a typical scanning rate of 30 nm/min. The raw SPV data were not corrected for the spectrum of the xenon lamp.

Results and Discussion

The importance of low-cost, efficient, large-area solar cells cannot be underestimated given their potential technological impacts in many applications. We present here strategies that allow us to prepare large areas of polymer−metal oxide *p*−*n* junctions, which show solar-induced photovoltage enhancement in most of the visible spectrum, especially in the red region. We choose a family of polythiophene, namely PT(4): poly(3-butylthiophene), PT(8): poly(3-octylthiophene), and PT(12): poly(3-dodecylthiophene, as the electrooptically active polymers. The controlled insulating layer is fabricated in a layer-by-layer manner by alternatively dipping the inorganic substrate in poly(styrene sulfonate) (PSS) and poly(diallydimethylammonium) (PDDA). The sequence of the self-assembled multilayer (SAM) insulator depends on the surface charge characteristics of the inorganic substrates. For example, titanium dioxide has positively charged sites on its surface, and hence we start with the formation of the PSS monolayer first. On the other hand, silica and indium tin oxide surfaces are negatively charged and we need to deposit PDDA first. Finally, the P3AT films were spun on either the self-organized PSS−PDDA multilayer or directly on the bare metal oxide substrates to finish the construction of organic−inorganic *p*−*n* or *p*−I−*n* junctions for photovoltage studies. The metal oxide films were prepared by polymer-solution deposition techniques, which are suitable for formation of large area metal oxide thin films. Their energy diagrams of inorganic materials relative to the organic semiconductive PT polymer is shown in Figure 1 to facilitate understanding of the charge-transfer phenomena discussed below.

1. Formation of Polaron at the PT−TiO_2 *p*−*n* Junction. To establish control experiments, we started with measuring bare SPV spectra for inorganic substrates only. For the TiO_2/ITO junction, we found two broad peaks, one centered at 650 nm with a photovoltage of ~20 mV and another at 375 nm with a peak value of 500 mV.[30] The low-energy photovoltaic response belongs to TiO_2's surface states and the high-energy band corresponds to the band-gap excitation of TiO_2. The onset of this broad SPV band starting at 450 nm was due to the distinct absorption mechanisms for photons with an energy level slightly below band-gap energy E_g. For example, a nonnegligible electric field was always associated with a significant surface charge region. Because subbandgap absorption was electric-field-assisted, it could be expected to blur the sharp onset of the absorption. Moreover, photoassisted charge transfer might take place between shallow states expanding the SPV band to include "tail states".

Figure 2 shows the SPV spectra from PT/TiO_2/ITO junctions, where PT represents poly(3-butylthiophene), poly(3-octylthiophene), or poly(3-dodecylthiophene). For the initial scan of all PT/TiO_2 junctions, there is little SPV response from 600 to 800 nm. In other words, the formation of the PT/TiO_2 interface erased the photovoltaic response from the surface states of TiO_2. For the PT(4)/TiO_2 junction, the onset of photovoltage begins at 600 nm and reaches the maximum at 365 nm. A broad SPV response, centered at 470 nm, is related to electron transfer from PT(4) to the TiO_2 surface. But, for PT(8)/TiO_2 and PT(12)/TiO_2 junctions, the onset of photovoltage response begins at 550 and 450 nm, respectively. Moreover, three vibronic peaks centered at 480 nm emerged, along with another shoulder band at 420 nm. The energy levels of PT and TiO_2 are shown in Figure 1. These bands can be attributed to the electron transfer from PT to TiO_2 as shown in Figure 3. The separated electron hole pairs recombine readily as soon as the light is turned off, when the excitation is below TiO_2 band gap. The fact that finer structures were observed in these bands indicates that PTs form

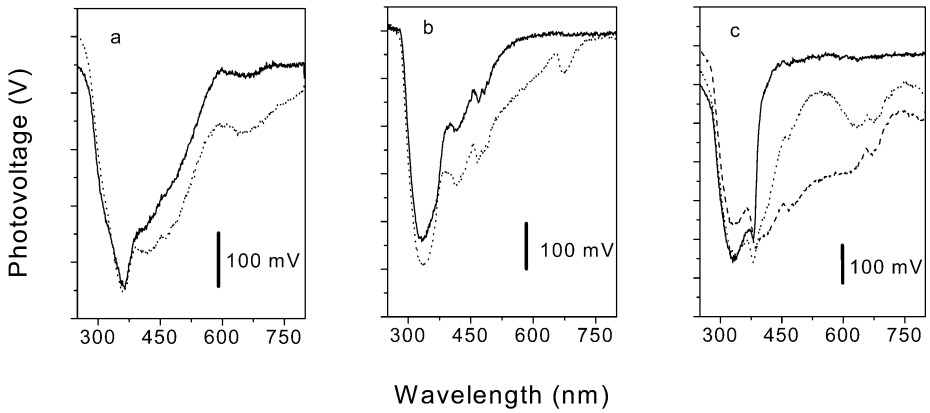

Figure 2. Surface photovoltage spectra of (a) PT(4)/TiO_2, (b) PT(8)/TiO_2, and (c) PT(12)/TiO_2. Solid lines are the first scan, dot lines are the second scan, and the dash line is the third scan for PT(12)/TiO_2 17 h after the initial scan.

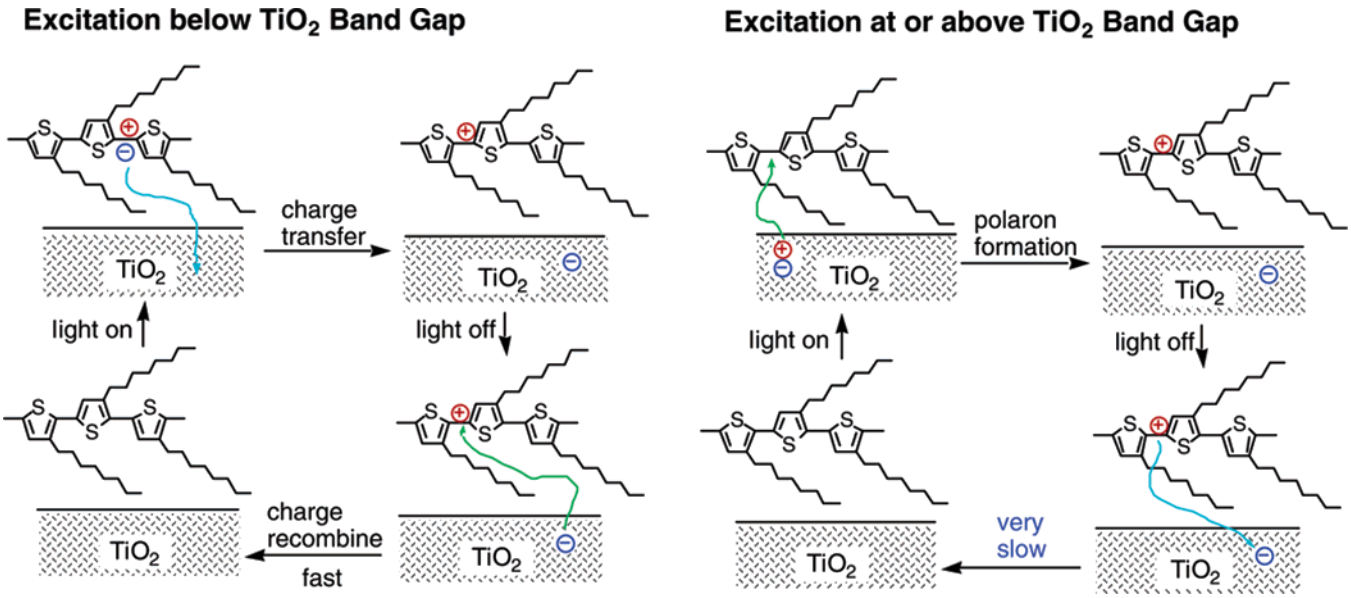

Figure 3. Systematic drawing of chemical structures of the PT polymer to illustrate the rapid reversible charge transfer when excited below the TiO_2 band gap and the mechanism of polaron formation at the inorganic−organic interface (IOI) heterojunctions of PT and TiO_2 when excited above the band gap.

a highly ordered lamellae structure. The strongest response between 340 and 380 nm is due to the optical absorption at the band-gap of TiO_2, followed by charge transfer at the PT−TiO_2 interface.

Of particularly interest is a new photovoltage band observed at 675 nm for the second scan of the PT(8)/TiO_2 junction and the PT(12)/TiO_2 junction, that is, after the excitation of TiO_2 band gap (Figures 3 and 4). For the second scan of the PT(4)/TiO_2 junction, a very broad SPV band was observed around this range with no well-defined peak maximum in the spectrum. Apparently, the first scan created some "trapped states" with an excitation energy at 675 nm (∼1.83 eV); this excitation energy matches remarkably well with polaron bands in PT. Therefore, we attribute these trapped states to be polaron states in PT. Janssen et al.[14] have recently reported photoinduced creation of cation radicals (polarons) in poly(*p*-phenylenevinylene) and polythiophene derivatives in contact with TiO_2, using photoinduced absorption spectroscopy and photoinduced ESR spectroscopy. Our SPV results provide direct spectral evidence that charge transfer from the PT polaron states to TiO_2 really happened at the IOI. If the first excitation scan stopped before the TiO_2 band gap, the polaron states would not be created. Only when the TiO_2 band gap was excited did the polaron band in PT became visible (Figures 3 and 4). Repeated scans between 900 nm and 500 nm on the same sample yielded no peak at 675 nm; this indicates that the photovoltage band is not due to the second-order scattered light at 337−340 nm. Had the second-order scattered light at 337−340 nm excited the samples, one would have observed the photovoltage signal at 675 nm in these control experiments. The charge carriers or polarons in the PT can delocalize over several monomeric units along the PT polymer chains, consistent with the high hole mobility.[31−33] The dashed line in Figure 2c shows the SPV response from the PT(12)/TiO_2 junction 17 h later. An overall enhancement of 150−300 mV photovoltage in the whole visible spectrum from 400 to 800 nm was observed. We believe that this enhancement was due to the continuous formation of polaron-like states in PT, which in turn gave rise to new photovoltage in the low energy end of the visible spectrum.

The control experiment of the PT(12)/ITO junction showed that there is no polaron formation or photovoltage enhancement from 400 to 800 nm after repeated optical excitation scans. This negative result suggests the importance of the PT/TiO_2 junction and the fact that formation of polaron is due to the migration of photoexcited holes from TiO_2 to PT.[31]

2. Polaron Lifetime. The lifetime of these polaron states depends on the length of the insulating alkyl side chains on PT. Figure 5 shows the time-dependent photovoltage response traces of PT(8)/TiO_2 and PT(12)/TiO_2 junctions in the spectra region from 600 to 750 nm. For the octyl side chains or PT(8), the lifetime was about several hours while monitoring the SPV signal at 675 nm. For a typical experiment, a 10-mV photovoltage response was measured after 4 h. As the length of the alkyl side chain increases from octyl to dodecyl, the lifetime of the polarons increases to several days. In a typical experiment, this photovoltage signal lasted 5 days. The measurement was carried out in such a way that the scan stopped at 600 nm to avoid further populating of the polaron states. For the short alkyl chains in PT(4), no polaron state with a well defined energy was observed, but enhanced SPV responses were still evident in the entire visible spectrum. These photoinduced photovoltage enhancements over the entire visible spectrum are really intriguing because one can envision a new generation of low-cost, highly effective, solid-state solar cells based on these IOI structures if, in the meantine, they can also provide high photocurrent. Nonetheless, harvesting photons in the low-energy region has been the critical challenge in designing new solar cells and polaron-like states in conjugated polymers may provide new opportunities for solving this problem.

3. The Dynamics of SPV Response. Analysis of photovoltage transients can determine the dynamic nature of interfacial states. Figure 6 shows an example of photodepopulation of surface states.[34] For the deep states, the thermal emission can be neglected and the electronic transitions involved in the transient consist of mostly photoinduced transitions from the surface state to the conduction band, at a rate of G^0, and the recombination transitions from the conduction band to the surface state, at a rate of R. Therefore, the concentration of the

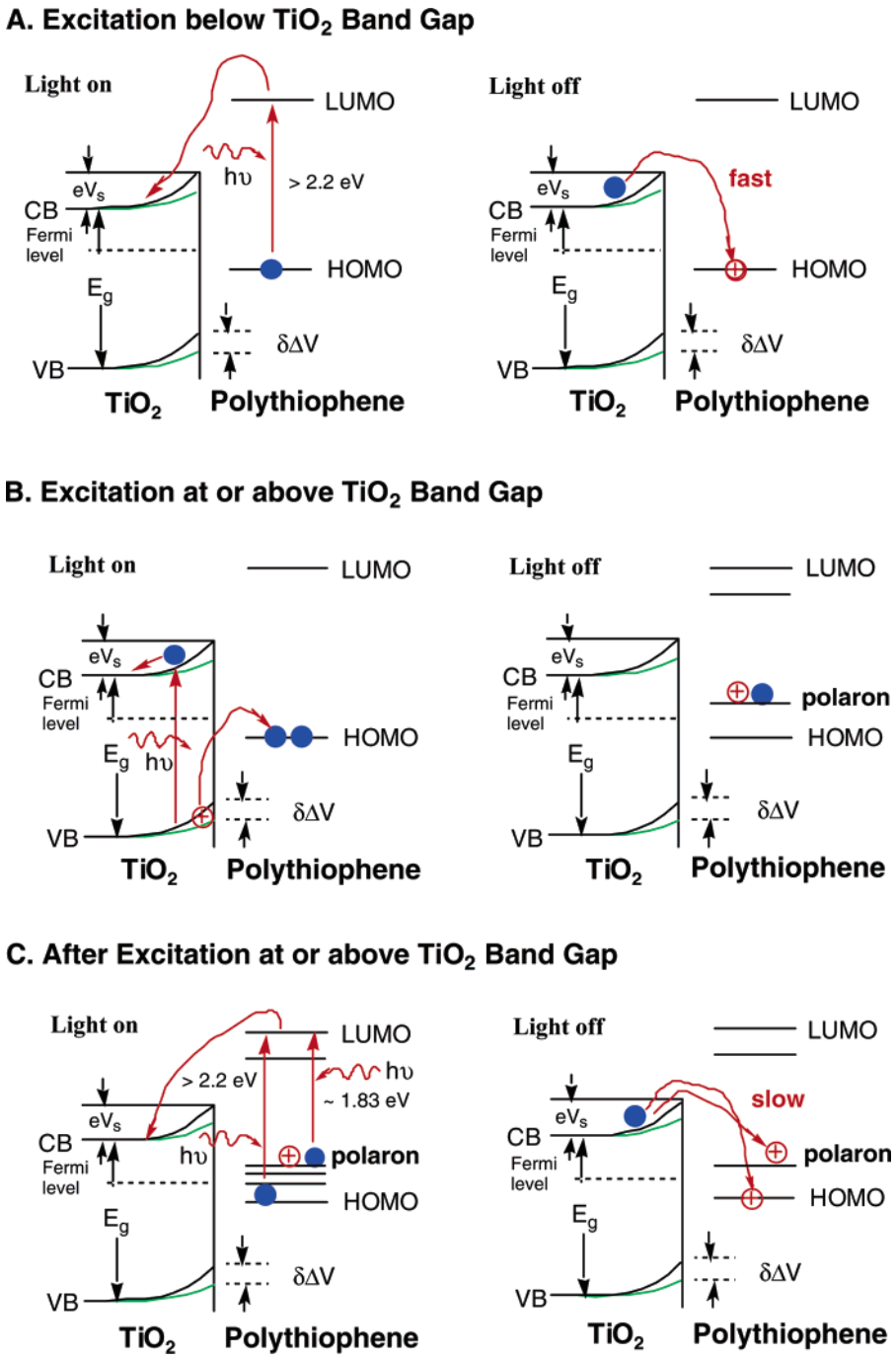

Figure 4. Systematic drawing of band structures of the PT polymer and TiO_2 to illustrate the rapid reversible charge transfer when excited below the TiO_2 band gap and the mechanism of polaron formation at the heterojunctions of PT and TiO_2 after the excitation at or above the TiO_2 band gap. Electronic energy levels are drawn relative to vacuum for PT's LUMO/HOMO and the TiO_2 valence band/conduction band.

electrons, n_t, on the surface state, E_t, varies according to the equation as given in (1).

$$dn_t/dt = R - G^0 \quad (1)$$

The initial increase of photovoltage for $t > t_0$ is due to G^0, which exceeds R_{ct}. Steady state is reached when $R = G^0$. This is achieved when the surface state population is depleted, thus decreasing the G^0 value. At the same time, R increases because the surface barrier diminishes and the concentration of empty states capable of capturing electrons grows. Since $G^0 = 0$ in the dark, recombination transitions, R, account for the photovoltage decay ($t > t_1$) entirely.

Figure 7 shows the SPV transient spectra of the PT(12)/TiO_2 junction excited at different wavelengths, namely at 335, 380, 420, 480, and 675 nm. For the excitation energy higher than the band gap of TiO_2 (e.g., at 335 and 380 nm), G^0 reaches its highest SPV response rapidly and then quickly decays to a steady response, displaying an initial sharp spike. When the light is turned off, SPV responses also rapidly drop back to the ground value. For the excitations below the TiO_2 band gap but higher than or at the LUMO−HOMO gap of PT (at 420 and 480 nm), G^0 also reaches a steady response quickly and maintains at that level. The light-off process is the same as those processes at 335 and 380 nm. When the light at 675 nm is turned on, however, a completely different character is observed in SPV

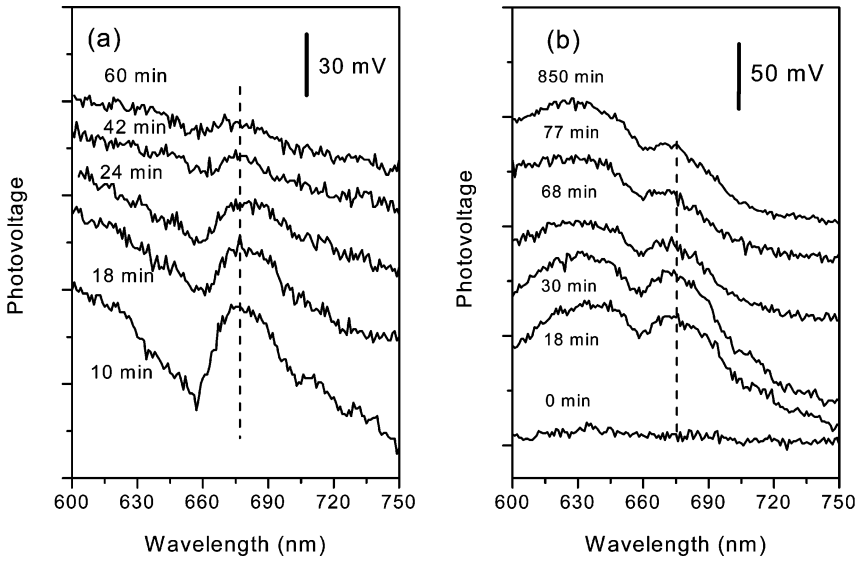

Figure 5. Series of temporal traces of the surface photovoltage (SPV) peak originated from the polaron state in the low energy region of the spectrum for (a) PT(8)/TiO_2 and (b) PT(12)/TiO_2. From these traces, the polaron lifetime at PT−TiO_2 junctions can be deduced. The scans stopped at 600 nm so that the polaron state formed at the PT(12)/TiO_2/ITO junction is not further populated.

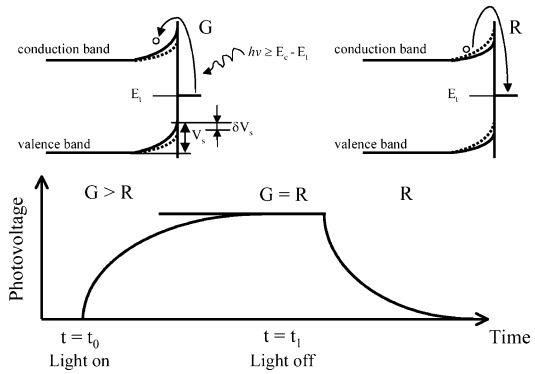

Figure 6. Surface photovoltage transient (lower portion) responses whose shape is governed by the nature of the original state. Schematic representation of the electron transitions from a surface state to the conduction band of TiO_2 (upper portion) under light illumination (G) and the reverse process in the dark (R).

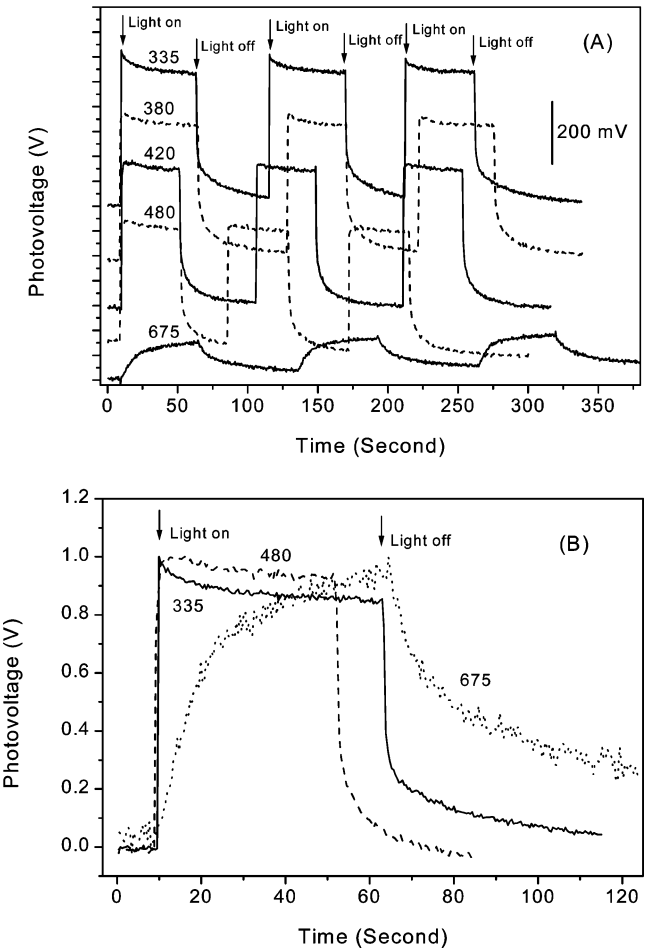

Figure 7. Surface photovoltage transient spectra of PT(12)/TiO_2 junction at different wavelengths (A). Note that excitation at either the TiO_2 band gap or the PT HOMO−LUMO transition yields transient spectra very different from that of exciting at the polaron band (B).

response. During the light-on process, G^0 increases very slowly and needs a long time to reach its highest value. Similarly, its SPV response also needs a long time to recover to zero when the light is turned off.

The different characteristics of these SPV responses indicate that electron/hole transfer come from different origins and perhaps goes through different routes. One is related to the TiO_2 band gap itself; another is related to the HOMO−LUMO excitation of PT, followed by electron transfer across IOI to TiO_2's conduction band. Both excitations are optically allowed and thus yield fast SPV responses. The low-energy SPV response, however, is produced from the excitation of PT's polaron states to PT's LUMO, followed by electron transfer across IOI to TiO_2's conduction band. The transition between polaron states and PT's LUMO is optically forbidden, and therefore this SPV band needs a longer time to reach the saturated photovoltage. Similarly, its reverse process is also slow. As a result, the photovoltage response related to the polaron state at 675 nm is only about 20% of the photovoltage generated at TiO_2's band gap or PT's HOMO to LUMO transitions.

4. Polaron Destruction and Recovery. It is well-known that a mild oxidizer such as I_2 can partially remove electrons from the PT valence band and hence exhibits a large iodine-doped conductivity (∼1350 S/cm), which is a dramatic increase from the undoped films (10^{-6} S/m). This dramatic increase of conductivity will alter the *p*−*n* junction to a metal−semiconductor junction. The polarons in conductive PT will therefore be more mobile and their excitation energies are less well

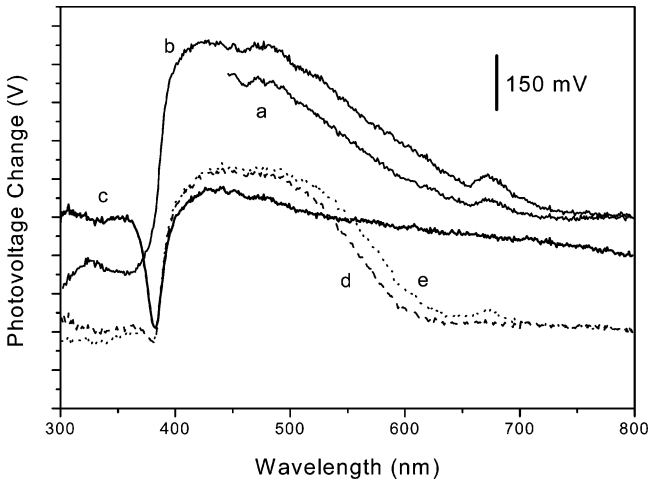

Figure 8. Difference surface photovoltage spectra show photoinduced enhancement at a PT(12)/TiO_2/ITO junction by rescanning a sample previously excited at TiO_2 band gap. (a) The first scan stopped at ~450 nm to avoid excitation of the TiO_2 band gap to confirm the existence of polaron states at 675 nm. (b) The second scan of the entire spectrum before exposure to I_2. (c) The third scan 2 min later after a brief exposure to I_2 vapor, (d) 20 min later, and (e) 40 min later.

defined.[35] Indeed, when a PT(12)/TiO_2 film was exposed to I_2 vapor for a few minutes, most of its SPV response was erased in the region between 400 and 800 nm (Figure 8, curve c), a region that originates from semiconductive PT rather than conductive PT. The polaron peak at 675 nm also disappeared completely. Interestingly, most SPV responses recovered ~20 min later (Figure 8, curves d and e) when the majority of iodides reversed back to I_2 and evaporated. After ~40 min, the polaron peak, although a little weaker, reappeared at 675 nm. Apparently, either the polarons created via photoexcitation of TiO_2 are very robust or I_2 vapor can also create the polarons' PT. In any case, the polaron states and photovoltage enhancement can only be observed at the *p*−*n* junction of PT/TiO_2, not a metal-semiconductor interface. Doping PT with other photo sensitive polymers such as poly (9-vinylcarbazole) does not significantly alter the photovoltage bands associated with polarons at 675 nm, vibronic peaks centered at 480 nm, and PT band gap at 420 nm.

5. Sunlight-enhanced Photovoltaic Effect. The real challenge is whether such photoinduced photovoltage enhancement due to the formation of polaron states can be generated with sunlight; this cannot be undervalued given the enormous technological importance of potential low-cost, efficient solar cells. In Figure 9, photoinduced enhancement of the photovoltage response is presented after a brief 2-min exposure of PT-(12)/TiO_2 film directly to sunlight. The enhancement of photovoltage was observed from the UV to the tail end of the visible spectrum (750 nm), demonstrating that a *p*−*n* junction made of PT and TiO_2 could be potentially useful in solid-state solar cells.

6. PT−SAM−TiO_2 *p*−*I*−*n* Junction. To further probe the formation of the polaron state in PT and its SPV properties, we inserted an insulating layer between PT and TiO_2 to form a *p*−*I*−*n* junction. Using a layer-by-layer self-assembly technique, we have deposited PDDA−PSS on TiO_2 films (~70 nm) supported by ITO substrates. Since TiO_2 surfaces have positively charged characters, the first anchoring layer is PSS and the terminating layer is PDDA. The insulating layer consists of six bilayers of PDDA−PSS. According to X-ray reflectivity studies, this layer is approximately 6 nm thick.[36,37] On top of the PDDA−PSS multilayer structure, we then spun a 50-nm thick

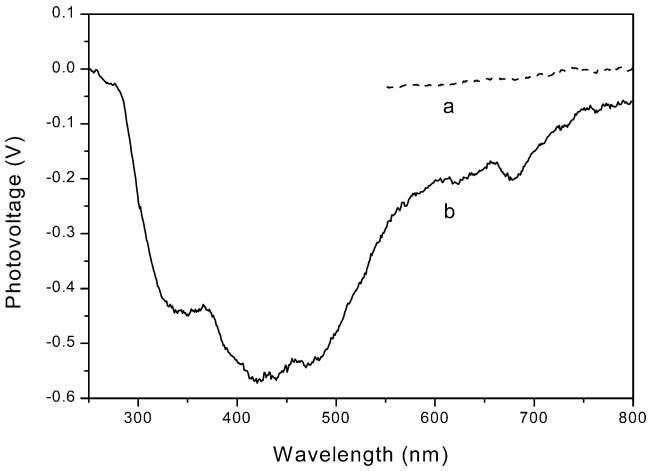

Figure 9. Surface photovoltage spectra of PT(12)/TiO_2/ITO (a) before exposure to sunlight and (b) after a brief exposure to sunlight for ~2 min. Photoinduced enhancement of photovoltage contributes to ~200 mV over most of the visible spectrum due to the formation of sunlight-induced polaron-like states.

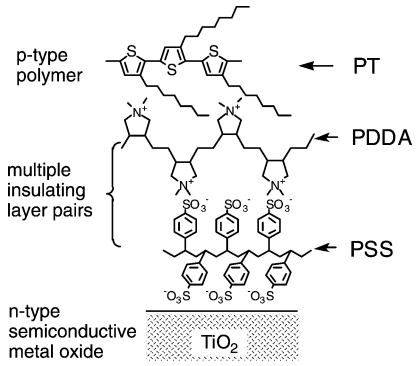

Figure 10. Schematic representation of insertion of a multilayer consisting of PSS and PDDA between the heterojunction of PT and TiO_2 to form a *p*−*I*−*n* junction.

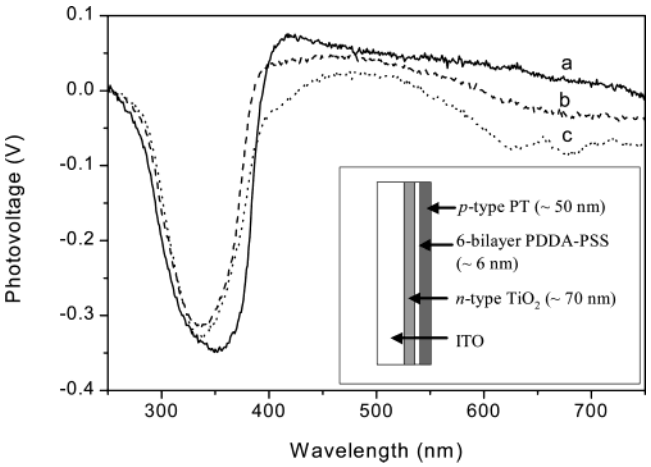

Figure 11. Surface photovoltage spectra of PT(12)/6-bilayer PDDA−PSS/TiO_2/ITO: (a) the first scan, (b) the second scan of the 6-bilayer PDDA-−PSS/TiO_2/ITO as a control experiment, and (c) the second scan of the PT(12)/6-bilayer PDDA−PSS/TiO_2/ITO, which shows photoinduced states at 675 nm. The inset is a side view of the layered structure for the PT(12)/6-bilayer PDDA−PSS/TiO_2/ITO junction.

PT(12) layer to fabricate a complex junction of PT(12)/(PDDA−PSS)$_6$/TiO_2 as shown in Figure 10. Figure 11 shows the SPV spectra of the complex junction along with spectra from PDDA−PSS/TiO_2 for comparison. In the first scan, no polaron excitation at 675 nm was observed. However, the TiO_2 band

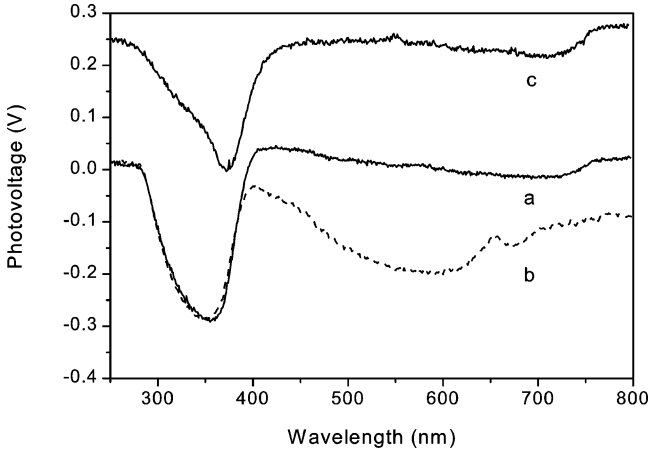

Figure 12. Surface photovoltage spectra of PT(12)/ZnO/ITO junction obtained from (a) the first scan, (b) the second scan, and (c) the bare ZnO/ITO. Similar to TiO_2/ITO systems, polaron states at 675 nm are generated after the initial excitation of ZnO band gap.

gap was excited. Can holes in TiO_2 penetrate six-layer pairs of PDDA−PSS and create polaron states in PT? In the second scan, the SPV peak related to polaron excitation appeared at 675 nm with a diminished intensity of 20 mV. This result suggests that holes can first penetrate a buffer layer as thick as 6 nm and hop into PT to create polaron states. Second, electrons from polaron excitation can again penetrate the 6-nm buffer layer and hop into the TiO_2 conduction band. On the contrary, SPV peaks centered at 480 nm and the broad band at 420 nm disappeared completely. This indicated that the PDDA−PSS buffer layer effectively blocked the electron transfer to TiO_2 associated with excitation of PT HOMO−LUMO but not the polaron state.

7. PT−Metal Oxide Junctions. To further investigate the generality of this polaron formation at the IOIs, we have studied other inorganic−organic junctions, including PT/ZnO, PT/$BaTiO_3$, PT/$SrTiO_3$, PT/HfO_2, and PT/CdS. By studying these junctions, we hope to shed light on the necessary conditions for generating polarons at IOIs. Furthermore, we would like to determine whether polaron-assisted photovoltage enhancement in the visible spectrum, as in the case of the PT−TiO_2 junction, is a general phenomenon.

Figure 12 shows the SPV spectra of the PT(12)/ZnO/ITO junction. To establish control experiments, we again first examined the junction of ZnO/ITO (Figure 11, curve c). A downward response means that ZnO is an *n*-type semiconductor. A 50-mV photovoltage response was observed at 750 nm, related to surface states of the ZnO film. No photovoltage response between 400 and 700 nm was observed. While exciting the band-gap of ZnO, the photovoltage increased dramatically at 400 nm and reached a peak value of 250 mV at 375 nm. For the PT(12)/ZnO junction, a broad SPV peak was observed at 355 nm in the first scan with an peak intensity of 350 mV. In the second scan, the polaron SPV peak located at 675 nm emerged. These results confirm that the origin of the SPV feature at 675 nm belongs to PT rather than the metal oxides. As with the polarons at the PT−TiO_2 junctions, these polaron states are also quite stable. Their SPV responses are still visible hours after the initial excitations of the inorganic semiconductor band gap. Figure 13 shows a series of time-dependent photovoltage spectra of the PT(12)/ZnO junction in the region from 550 to 750 nm. The measurement was carried out in such a way that the scan was stopped at 550 nm to avoid further populating the polaron states. For the PT(12)/ZnO junction, a 10-mV photovoltage response was measured after 2 h. As more time elapsed,

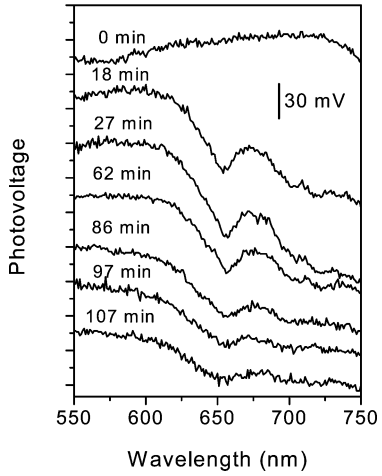

Figure 13. Temporal traces of the surface photovoltage (SPV) polaron band, which was created by the excitation of ZnO band gap. The scans stopped at 550 nm so that the polaron state formed at the PT(12)/ZnO/ITO junction is not further populated. The lifetime of polarons at the PT(12)/ZnO/ITO junctions is approximately ∼2 h.

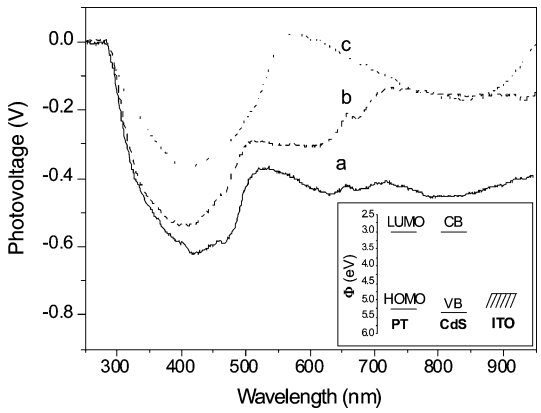

Figure 14. Surface photovoltage spectra of a PT(12)/CdS/ITO junction obtained from (a) the first scan and (b) the second scan. Surface photovoltage spectra of the bare CdS/ITO (c). The inset is the electronic energy level diagram relative to vacuum for PT (LUMO: lowest unoccupied molecular orbital; HOMO: highest occupied molecular orbital), CdS (VB: valence band; CB: conduction band), and ITO.

the polaron SPV response became broader and broader, due to back electron transfer from PT(12) to ZnO.

For comparison purposes, we have also studied the junctions between PT and insulating metal oxides. For the control $BaTiO_3$/ITO junction, there has been only one band at 345 nm with an intensity of 250 mV. For the heterojunction PT(12)/$BaTiO_3$, we again only observed the same SPV peak, indicating the IOI junction was not active in contributing photovoltage. Repeated scans generated no polaron SPV peak; the only change was the contact potential drift from 100 mV to 0 mV due to the formation of a polymer layer. Similar results have also been obtained from other PT-insulator junctions, such as PT/$SrTiO_3$ and PT/HfO_2.

Finally, we measured the SPV spectra of the *p*-type PT(12)/*n*-type CdS junction. These spectra are shown in Figure 14. For control CdS films, we observed two broad SPV responses: one located at 840 nm, which belongs to surface states of CdS, and another located at 420 nm, which originates from the band gap of CdS. After coating CdS with a layer of PT(12), photovoltage enhancement was observed in the whole spectrum, ranging from 300 to 950 nm. The SPV peak located at 675 nm, which related to polarons in PT, can be observed even in the first scan. The band gap of CdS is about 2.4 eV and it has similar energy levels

to those in PT. This matching in energy levels produces strong interactions between PT and CdS and facilitates charge transport, even under the room light illumination. For the first scan, polaron and polaron-like states have been created already. In the initial scan, we observed about 400 mV SPV enhancement at 950 nm. In the second and subsequent scans, this SPV enhancement remained at ~200 mV at 950 nm. These results indicate that PT/CdS junctions also have the overall photoinduced enhancement of photovoltage in the visible spectrum.

Conclusions

In summary, we have found that photoinduced charge transfer readily occurred at the organic *p*-type PT and inorganic *n*-type semiconductive TiO_2, ZnO, and CdS interfaces. Polarons can be generated in PT polymer backbones as a result of photoexcitation of *n*-type inorganic semiconductors, followed by hole migration to the conjugated polymer. The lifetime of these polarons depends on the length of the insulating alkyl side chains on PT backbones and can last as long as a few days. When a buffer layer was inserted between PT and TiO_2 junctions, the photovoltage responses originated from excitation of the HOMO to LUMO transition in PT disappeared. However, SPV responses due to the polaron states can still be found at 675 nm. It is the polaron states and/or polaronlike states in PT that are responsible for the photoinduced photovoltage enhancement in the whole visible spectrum when compared to bare TiO_2 and ZnO films. For PT-coated CdS films, the photoinduced photovoltage enhancement can be extended from 400 nm into the near-IR region of 950 nm. For PT−insulator junctions such as PT/$BaTiO_3$, neither photoinduced polaron states nor photoinduced photovoltage enhancement was observed, indicating that the *p*−*n* character at the IOI is important for generation of polaron states and photoinduced photovoltage enhancement. The significance of this study is that large-area photovoltaic cells made of low-cost conductive polymers and metal oxides or metal sulfides may have potential uses in harvesting solar energy.

Acknowledgment. We acknowledge the support of the US Department of Energy (DOE), Office of Basic Energy Sciences: Division of Materials Science and Engineering and DOE-Los Alamos, subcontract (28893-001-01-35). A.D.Q.L. is a Beckman Young Investigator (BYI) and thanks the support of the Arnold and Mabel Beckman Foundation.

References and Notes

(1) Friend, R. H.; Gymer, R. W.; Holmes, A. B.; Burroughes, J. H.; Marks, R. N.; Taliani, C.; Bradley, D. D. C.; Dos Santos, D. A.; Bredas, J. L.; Logdlund, M.; Salaneck, W. R. *Nature* **1999**, *397*, 121.
(2) Tang, C. W. *Appl. Phys. Lett.* **1986**, *48*, 183.
(3) Rosseinsky, D. R.; Mortimer, R. J. *Adv. Mater.* **2001**, *13*, 783.
(4) Chang, S. C.; Liu, J.; Bharathan, J.; Yang, Y.; Onohara, J.; Kido, J. *Adv. Mater.* **1999**, *11*, 734.
(5) de Morais, T. D.; Chaput, F.; Lahlil, K.; Boilot, J.-P. *Adv. Mater.* **1999**, *11*, 107.
(6) Bao, Z. *Adv. Mater.* **2000**, *12*, 227.
(7) Ho, P. K. H.; Thomas, D. S.; Friend, R. H.; Tessler, N. *Science* **1999**, *285*, 233.
(8) O'Regan, B.; Grätzel, M. *Nature* **1991**, *353*, 737.
(9) Nazeeruddin, M. K.; Kay, A.; Rodicio, I.; Humpbry-Baker, R.; Miiller, E.; Liska, P.; Vlachopoulos, N.; Grätzel, M. *J. Am. Chem. Soc.* **1993**, *115*, 6382.
(10) Bach, U.; Lupo, D.; Comte, P.; Moser, J. E.; Weissörtel, F.; Salbeck, J.; Spreitzer, H.; Grätzel, M. *Nature* **1998**, *395*, 583.
(11) Boschloo, G.; Fitzmaurice, D. *J. Phys. Chem. B* **1999**, *103*, 2228.
(12) Bäubleer, T. K.; Glowacki, I.; Scherf, U.; Ulanski, J.; Hörhold, H. H.; Neher, D. *J. Appl. Phys.* **1999**, *86*, 6915.
(13) Kajihara, K.; Tanaka, K.; Hirao, K.; Soga, N. *Jpn. J. Appl. Phys.* **1997**, *36*, 5537.
(14) van Hal, P. A.; Christiaans, M. P. T.; Wienk, M. M.; Kroon, J. M.; Janssen, R. A. J. *J. Phys. Chem. B* **1999**, *103*, 4352.
(15) Arango, A. C.; Johnson, L. R.; Bliznyuk, V. N.; Schesinger, Z.; Carter, S. A.; Hörhold, H. H. *Adv. Mater.* **2000**, *12*, 1689.
(16) Breeze, A. J.; Schlesinger, Z.; Carter, S. A.; Brock, P. J. *Phys. Rev. B* **2001**, *64*, 125205.
(17) Gebeyehu, D.; Brabec, C. J.; Sariciftci, N. S.; Vangeneugden, D.; Kiebooms, R.; Vanderzande, D.; Kienberger, F.; Schindler, H. *Synth. Met.* **2002**, *125*, 279.
(18) Huisman, C. L.; Goossens, A.; Schoonman, J. *J. Phys. Chem. B* **2002**, *106*, 10578.
(19) Luzzati, S.; Basso, M.; Catellani, M.; Brabec, C. J.; Gebeyehu, D.; Sariciftci, N. S. *Thin Solid Films* **2002**, *403*−*404*, 52.
(20) Stathatos, E.; Lianos, P.; Laschewsky, A.; Ouari, O.; van Cleuvenbergen, P. *Chem. Mater.* **2001**, *13*, 3888.
(21) Sayama, K.; Tsukagoshi, S.; Hara, K.; Ohga, Y.; Shinpou, A.; Abe, Y.; Suga, S.; Arakawa, H. *J. Phys. Chem. B* **2002**, *106*, 1363.
(22) Sicot, L.; Geffroy, B.; Lorin, A.; Raimond, P.; Sentein, C.; Nunzi, J.-M. *J. Appl. Phys.* **2001**, *90*, 1047.
(23) Meijer, E. J.; Mangnus, A. V. G.; Hart, C. M.; de Leeuw, D. M.; Klapwijk, T. M. *Appl. Phys. Lett.* **2001**, *78*, 3902.
(24) Kronik, L.; Shapira, Y. *Surf. Sci. Rep.* **1999**, *37*, 1.
(25) Baikie, I.; Petermann, U.; Lägel B. *Surf. Sci.* **1999**, *433*−*435*, 249.
(26) Lägel B.; Baikie, I. D.; Petermann U. *Surf. Sci.* **1999**, *433*−*435*, 622.
(27) Li, L. S.; Zhang, J.; Wang. L. J.; Chen, Y.; Hui, Z.; Li, T. J.; Chi, L. F.; Fuchs, H. *J. Vac. Sci. Technol., B* **1997**, *15*, 1618.
(28) Gai, D.; Mastai, Y.; Hodes, G.; Kronik, L. *J. Appl. Phys.* **1999**, *86*, 5573.
(29) Shalish, I.; Shapria, Y.; Burstein, L.; Salzman, J. *J. Appl. Phys.* **2001**, *89*, 390.
(30) Li, L. S.; Jia, Q. X.; Li, A. D. Q. *Chem. Mater.* **2002**, *14*, 1159.
(31) Sirringhaus, H.; Brown, P. J.; Friend, R. H.; Nielsen, M. M.; Bechgaard, K.; Langeveld-Voss, B. M. W.; Spiering, A. J. H.; Janssen, R. A. J.; Meijer, E. W.; Herwig, P.; de Leeuw, D. M. *Nature* **1999**, *401*, 685.
(32) Brown, P. J.; Sirringhaus, H.; Harrison, M.; Shkunov, M.; Friend, R. H. *Phys. Rev. B* **2001**, *63*, 125204.
(33) Österbacka, R.; An, C. P.; Jiang, X. M.; Vardeny, Z. V. *Science* **2000**, *287*, 839.
(34) Lagowski, J. *Surf. Sci.* **1994**, *299/300*, 92.
(35) Chen, T. A.; Rieke, R. D. *Synth. Met.* **1993**, *60*, 175.
(36) Li, L. S.; Wang, R.; Fitzsimmons, M.; Li, D. Q. *J. Phys. Chem. B* **2000**, *104*, 11195.
(37) Lütt, M.; Fitzsimmons, M.; Li, D. Q. *J. Phys. Chem. B* **1998**, *102*, 400.